

# Types and dimensionality of magnetic order in high- $T_c$ superconductors of the $\text{YBa}_2(\text{Cu}_{1-x}\text{Fe}_x)_3\text{O}_y$ system

I. S. Lyubutin and T. V. Dmitrieva

*Institute of Crystallography, Russian Academy of Sciences, 117333 Moscow, Russia*

(Submitted 3 September Month 1993)

Zh. Eksp. Teor. Fiz. **105**, 954–966 (April 1994)

Mössbauer spectroscopy has been used to study the temperature dependence of the hyperfine magnetic fields  $H_{\text{hf}}$  at  $^{57}\text{Fe}$  nuclei in various structural positions in high- $T_c$  compounds with the general formula  $\text{YBa}_2(\text{Cu}_{1-x}\text{Fe}_x)_3\text{O}_y$  in superconducting and semiconducting states. Analysis of the  $H_{\text{hf}}(T)$  curves on the basis of various theoretical models shows that the magnetic order of the iron ions (in a semiconducting state) in Cu2 sites is three-dimensional, while 2D and 3D magnetic orders can exist in Cu1 sites. A spin-glass state is also possible, depending on the local oxygen coordination of the iron ion and on the temperature. A crossover of the magnetic-order parameter is observed in the temperature interval 150–200 K. The existence of a 3D magnetic order in the Cu1 sites of superconducting samples means that the 3d electrons of Cu2–O layers, which are responsible for the superconductivity, may simultaneously participate in an exchange interaction between two magnetic Cu1–O layers.

## 1. INTRODUCTION

Several studies<sup>1–8</sup> of the  $\text{YBa}_2\text{Cu}_3\text{O}_y$  system doped with iron ions have revealed that magnetic order and superconductivity can coexist for iron ions in Cu1 sites. It follows from simple structural considerations that magnetic order in the coexistence region must be quasi-two-dimensional (2D), since the exchange interaction between two Cu1–O layers which is necessary for a three-dimensional (3D) order would require that the superconducting Cu2–O layer be involved in this interaction.<sup>9</sup> It is possible that a layered structure of a new type is realized in an iron-doped 1-2-3 phase. In this new type of layered structure, superconducting layers in  $ab$  planes ( $z=1/3$ ) would alternate along the  $c$  axis with magnetic layers in the Cu1–O  $ab$  basal ( $z=0$ ) planes. An experimental study of the dimensionality of the magnetic order becomes a matter of fundamental importance here, since in the case of 3D order the 3d electrons of the Cu2–O layers, which are responsible for the superconductivity, should simultaneously participate in an exchange interaction between the two nearest magnetic Cu1–O layers.

In this paper we are reporting a study by Mössbauer spectroscopy of the temperature dependence of the hyperfine magnetic fields  $H_{\text{hf}}$  at the nuclei of iron ions in Cu1 and Cu2 sites of the  $\text{YBa}_2(\text{Cu}_{1-x}\text{Fe}_x)_3\text{O}_y$  system. The behavior  $H_{\text{hf}}=f(T)$  is analyzed on the basis of certain models with the goal of determining the type and dimensionality of the magnetic order for the iron ions, both in Cu2 sites and in Cu1 sites with various oxygen surroundings.

## 2. EXPERIMENTAL PROCEDURE AND ANALYSIS OF RESULTS

From the series  $\text{YBa}_2(\text{Cu}_{1-x}\text{Fe}_x)_3\text{O}_y$  we selected six samples, which correspond to the most typical situations: three oxygen-saturated samples ( $y \geq 7$ ) and three oxygen-depleted ones ( $y < 6.5$ ), with  $x=0.01, 0.10$ , and  $0.23$ . Two

of the oxygen-saturated samples were superconductors, with  $T_c=92$  K for  $x=0.01$  and  $T_c=39$  K for  $x=0.10$ . In the third ( $x=0.23$ ), the superconductivity was suppressed by doping, and the sample exhibited semiconducting conductivity down to  $T=4.2$  K. The conductivity of the oxygen-depleted samples was also typical of semiconductors. The procedure for synthesizing and characterizing the test samples is described in detail in Refs. 10 and 11.

Mössbauer spectra of  $^{57}\text{Fe}$  nuclei were recorded on a standard spectrometer in the geometry in which the  $\gamma$  rays passed through the test sample, over the temperature range 4.6–500 K.

In the magnetic-order region, the Mössbauer spectra, split by the Zeeman interaction, were deciphered by special computer programs<sup>11,12</sup> into constituent subspectra  $M_i$  ( $i=1,2,\dots$ ) corresponding to different structural positions of the iron ions: to Cu1 sites with oxygen coordination numbers  $k=4, k=5$ , and  $k=6$  and to Cu2 sites with  $k=5$ . Figures 1 and 2 show some typical spectra at low temperatures and the procedure for decomposing them into subspectra. The spectrum decomposition procedure is discussed in detail in Refs. 11–13, as is the assignment of the subspectra to the various structural positions. Using these results, we plotted the temperature dependence of the hyperfine magnetic fields,  $H_{\text{hf}}(M_i)=f(T)$  at the nuclei of the iron ions in various structural positions. Then assuming that the field  $H_{\text{hf}}$  at the nucleus of a given ion is proportional to its magnetic moment, we carried out a computer analysis of these curves, using the following theoretical approximations:

- a critical coefficient model,

$$H_{\text{hf}}=H_0(1-T/T_N)^\beta, \quad (1)$$

- a 2D Ising model,

$$H_{\text{hf}}=H_0(1-x^{-2})^{1/8}, \quad (2)$$

where  $x=\sinh(2J_1/kT)\sinh(2J_2/kT)$ , and

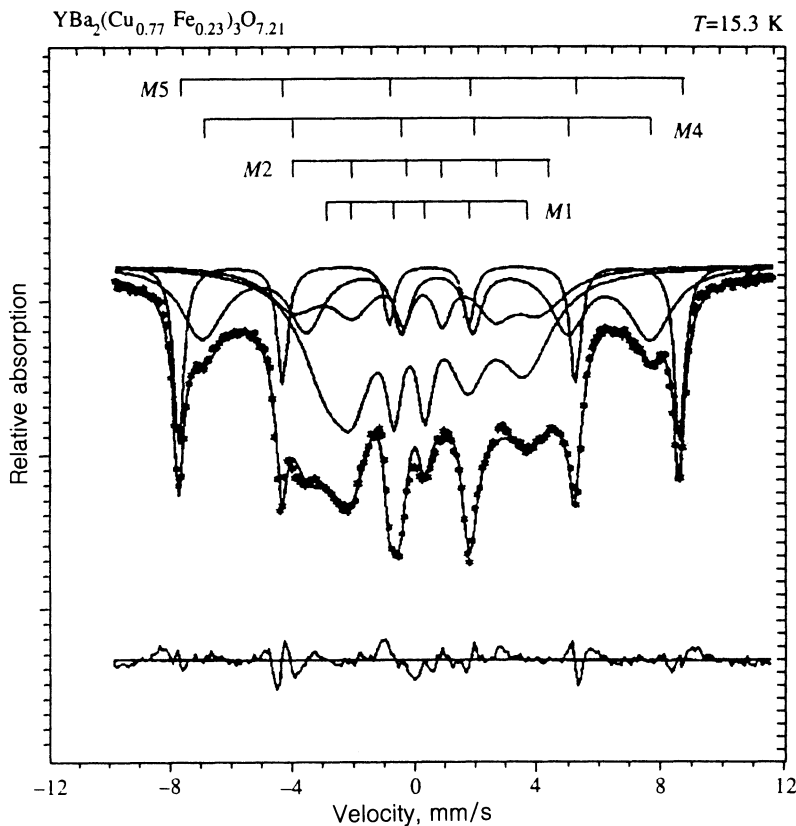


FIG. 1. Mössbauer spectrum of a  $\text{YBa}_2(\text{Cu}_{0.77}\text{Fe}_{0.23})_3\text{O}_{7.21}$  sample at  $T=15.3$  K. Also shown here is a computer decomposition of the spectrum into four six-line components  $M1$ ,  $M2$ ,  $M4$ , and  $M5$ . The signal representing the decomposition error is shown at the bottom.

- a molecular field model (a Brillouin function),

$$H_{\text{hf}} = H_0 B_s \{ [3S/(S+1)] h/t \}, \quad (3)$$

where  $h = H_{\text{hf}}/H_0$  and  $t = T/T_N$ .

Here  $H_0$  is the value of  $H_{\text{hf}}$  in the limit  $T \rightarrow 0$ ,  $J_1$  and  $J_2$  are the values of the exchange integrals in the  $x$  and  $y$  directions in the Ising model, and  $S$  is the spin of an iron ion. The following parameters were varied in the course of the analysis:  $\beta$ ,  $H_0$ , and  $T_N$  in expression (1);  $H_0$ ,  $J_1$ , and  $J_2$  in (2); and  $H_0$ ,  $S$ , and  $T_N$  in (3).

### 3. EXPERIMENTAL RESULTS

#### 3.1. Oxygen-rich samples

The superconducting samples exhibit only a single, low-temperature magnetic phase transition, at  $T_{m1} \approx 3.3$  and  $16$  K for  $x=0.01$  and  $0.1$ , respectively.<sup>14,15</sup> Figure 3, a and b, shows the temperature dependence of the fields  $H_{\text{hf}}$  for the three spectral components  $M1$ ,  $M2$ , and  $M4$ , which correspond to Cu1 sites in a  $\text{YBa}_2(\text{Cu}_{0.9}\text{Fe}_{0.1})_3\text{O}_{7.07}$  sample. The components are numbered in order of increasing value of the field at  $T=4.6$  K:  $H_{\text{hf}}(M1) \approx 210$  kOe,  $H_{\text{hf}}(M2) \approx 260$  kOe, and  $H_{\text{hf}}(M4) \approx 465$  kOe. The component  $M3$ , with the field  $H_{\text{hf}} \approx 360$  kOe, arises only after oxygen is removed. The component  $M5$ , with  $H_{\text{hf}} \approx 510$  kOe, is characteristic of iron ions in Cu2 sites.

Analysis of the  $H_{\text{hf}}(M4) = f(T)$  dependence on the basis of model (1) points unambiguously to the 2D nature of the magnetic order for sites of this type. The value of the critical coefficient,  $\beta=0.12$ , is essentially the same as the classical theoretical value  $\beta=0.125$  for an ideal 2D

model.<sup>16</sup> Analysis on the basis of the Ising model confirms this conclusion: The experimental points are described well by the theoretical curve for the 2D case with  $J_1=J_2$  and  $T_N=15$  K. We can then use the relation  $T_N=2.27J$ , which holds for the 2D Ising model, to calculate the exchange integral:  $J_1=J_2 \approx 6.61$  K. For the quasi-1D approximation, the theoretical curve does not agree as well with experiment (Fig. 3a). For  $M2$ , analysis on the basis of model (1) yields the value  $\beta=0.35$ , which is characteristic of a 3D order (Fig. 3b). The value of  $T_N$  is again close to  $15$  K. The  $H_{\text{hf}}(M2)$  curve can also be described by a Brillouin function. The dependence  $H_{\text{hf}}(M1) = f(T)$  is very nearly linear, with a value  $\beta=0.86$ . Interestingly, the value found for  $T_N$  from the extrapolation  $H_{\text{hf}} \rightarrow 0$  yields a value of  $T_N$  for the  $M4$  and  $M2$  components which is slightly too high,  $\approx 20$  K.

In the  $\text{YBa}_2(\text{Cu}_{0.77}\text{Fe}_{0.23})_3\text{O}_{7.21}$  sample, in which the superconductivity is suppressed by the high iron concentration, two phase transitions are observed:<sup>12</sup> a low-temperature one at  $T_{m1} \approx 30$  K and a high-temperature one at  $T_{m2} \approx 390$  K (Fig. 4). The low-temperature transition is exhibited by the component  $M4$  and by the resultant curve found by adding components  $M1$  and  $M2$ . The high-temperature transition is associated with  $M5$ . Analysis shows (Fig. 4) that the  $H_{\text{hf}}(M4)$  curve can be described well by the 2D models: by model (1) with  $\beta=0.11$  and  $T_N=29.4$  K and by model (2) with  $T_N=29.25$  K and  $J_1=J_2=12.9$  K. The  $H_{\text{hf}}(M1+M2)$  curve satisfies Eq. (1) with the 3D value  $\beta=0.39$  and  $T_N=29.5$  K. Analysis of the  $H_{\text{hf}}(M5) = f(T)$  dependence on the basis of model (1) yields  $\beta=0.35$ , which corresponds to 3D order. The

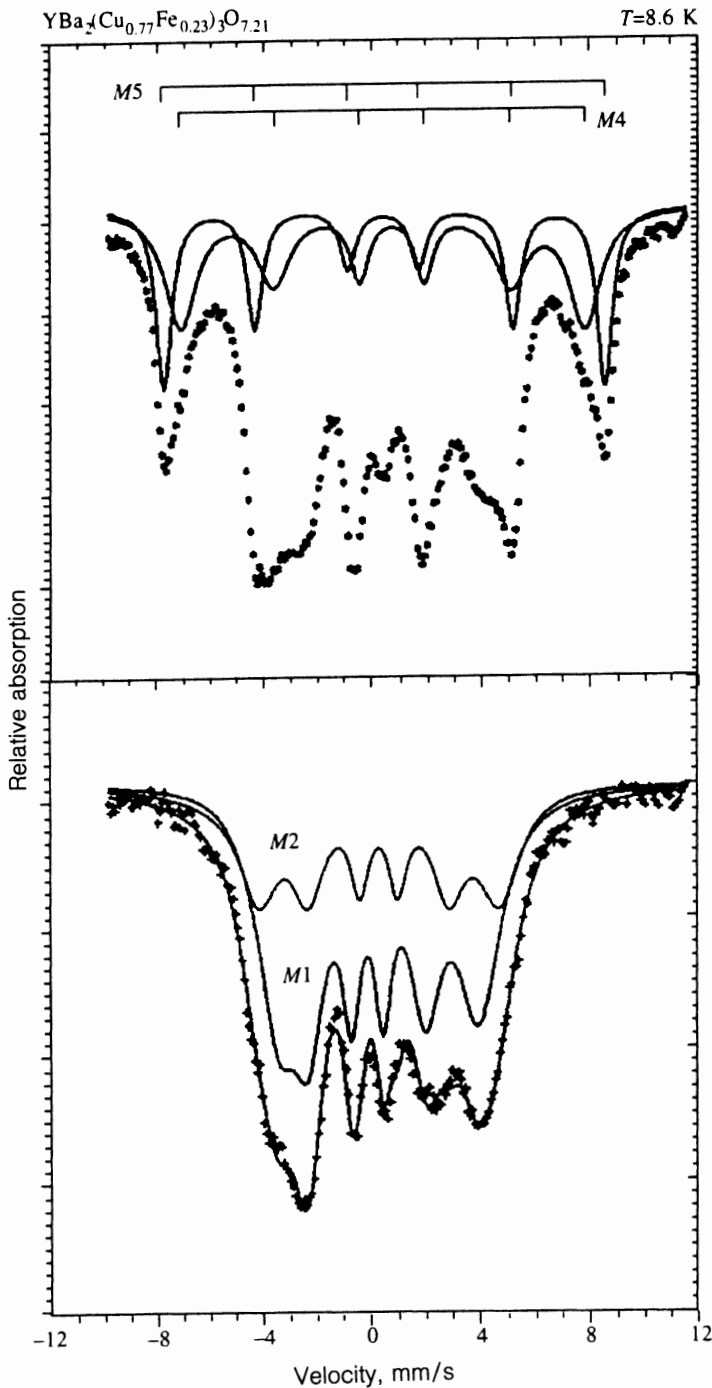


FIG. 2. Procedure for analyzing a spectrum through subtraction of individual Mössbauer components. Shown at the top of this figure is an experimental Mössbauer spectrum of a  $\text{YBa}_2(\text{Cu}_{0.77}\text{Fe}_{0.23})_3\text{O}_{7.21}$  sample at  $T=8.6$  K (the asterisks). Shown at the bottom is the difference spectrum for the same sample (the plus signs) after subtraction of components  $M4$  and  $M5$  from the original spectrum.

experimental points for  $M5$  also conform well to a Brillouin curve [model (3)] with a spin  $S=5/2$ .

### 3.2. Oxygen-poor samples

The semiconducting samples  $\text{YBa}_2(\text{Cu}_{0.9}\text{Fe}_{0.1})_3\text{O}_{6.36}$  and  $\text{YBa}_2(\text{Cu}_{0.77}\text{Fe}_{0.23})_3\text{O}_{6.49}$  exhibit only a single phase transition,<sup>17</sup> the high-temperature one, at  $T_{m2} \approx 460$  K (Figs. 5 and 6). The Mössbauer spectrum of each sample can be decomposed into four components:  $M2$ ,  $M3$ ,  $M4$ , and  $M5$ . The component  $M1$ , with  $H_{\text{hf}} \approx 210$  kOe, is not found in these test samples. However, a new component,  $M3$ , with a field  $H_{\text{hf}} \approx 350$  kOe, appears.

The temperature dependence of the fields  $H_{\text{hf}}$  is approximately the same for  $M4$  and  $M5$ . For the sample with

$x=0.1$  the two curves intersect at  $\sim 250$  K (Fig. 5). Analysis on the basis of model (1) yields  $\beta(M5)=0.41$  with  $T_N=453$  K and  $\beta(M4)=0.23$  with  $T_N=432$  K. In the sample with  $x=0.23$  the values of  $\beta$  for  $M5$  and  $M4$  are 0.35 and 0.31, respectively, with the common value  $T_N=460$  K (Fig. 6).

The  $H_{\text{hf}}=f(T)$  curves for  $M2$  and  $M3$  have similar shapes (Figs. 5 and 6). At a certain intermediate temperature the two curves merge and go through anomalous slope changes; the magnetic ordering moves off to the point  $T_{m2}$ . A similar  $H_{\text{hf}}(T)$  dependence was observed in Ref. 18 at impurity Fe nuclei in Cu1 sites for a  $\text{YBa}_2\text{Cu}_{2.2}\text{Co}_{0.8}\text{O}_y$  sample. We attempted to analyze those curves by partitioning the temperature range into several regions. For the

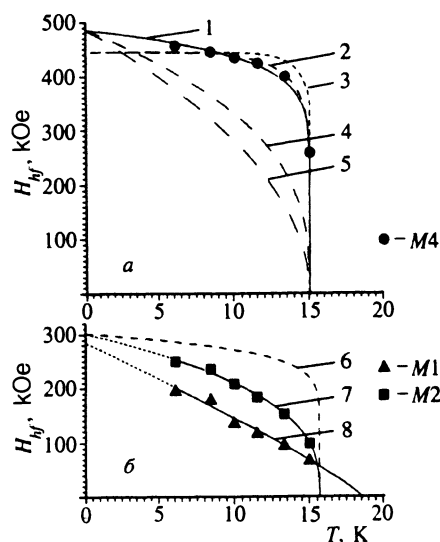


FIG. 3. Experimental and theoretical temperature dependence of the hyperfine magnetic fields  $H_{hf}(Mi)$  for various components of the Mössbauer spectrum in a  $YBa_2(Cu_{0.9}Fe_{0.1})_3O_{7.07}$  superconducting sample. A: Component  $M4$ . The circles show experimental points. 1,4,5—Theoretical curves calculated from model (1) for  $\beta$  values of 0.12, 0.35, and 0.5, respectively; 2,3—theoretical curves calculated from model (2) with  $J_1=J_2$  and  $J_1/J_2=10^{-3}$ , respectively. B: Experimental data. The triangles correspond to component  $M1$ , and the squares to component  $M2$ . 6,7—Theoretical curves calculated from model (1) for  $M2$  for  $\beta$  values of 0.12 and 0.35, respectively; 8—theoretical curve calculated from model (1) for  $M1$  and the value  $\beta=0.86$ .

sample with  $x=0.1$ , the  $H_{hf}(M3)$  curve is linear with  $\beta=1$  in the low-temperature region, and the  $H_{hf}(M2)$  curve can be described by a 2D model as in (2) with  $T_N=170$  K and  $J_1=J_2=75$  K. The high-temperature region for both  $M2$

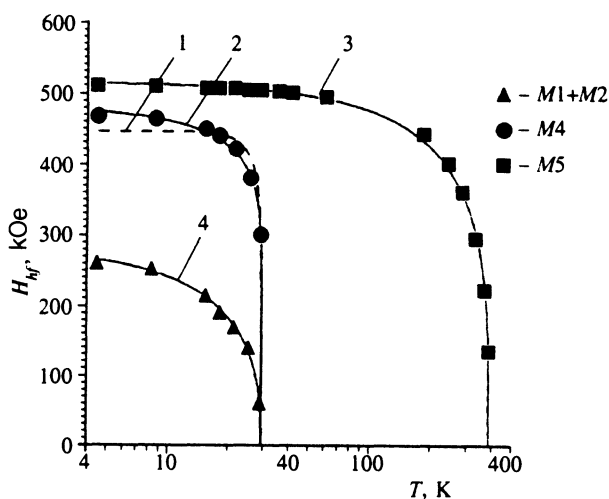


FIG. 4. Temperature dependence of the fields  $H_{hf}(Mi)$  for a  $YBa_2(Cu_{0.77}Fe_{0.23})_3O_{7.21}$  sample. The points are experimental. Triangles—The component  $M1+M2$ ; circles— $M4$ ; squares— $M5$ . The curves are theoretical. 1—2D Ising model, (2), for  $M4$ ; 2—model (1) for  $M4$  with  $\beta=0.11$ ; 3—model (1) for  $M5$  with  $\beta=0.35$ ; 4—model (1) for  $M1+M2$  with  $\beta=0.39$ . The temperature scale is logarithmic.

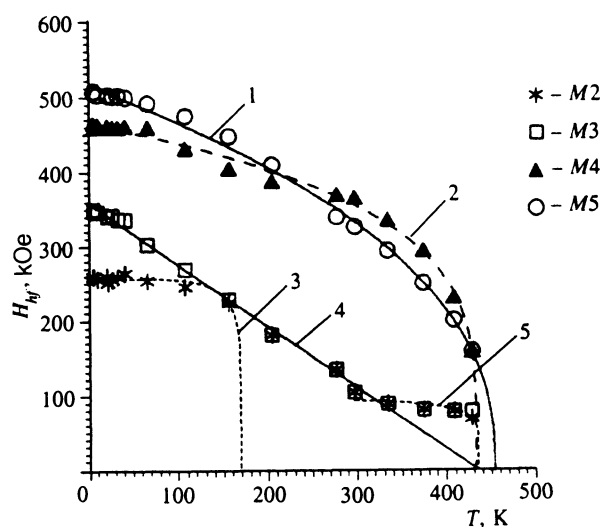


FIG. 5. Temperature dependence of the fields  $H_{hf}(Mi)$  for a  $YBa_2(Cu_{0.9}Fe_{0.1})_3O_{6.36}$  sample. The points are experimental. Asterisks—Component  $M2$ ; squares— $M3$ ; triangles— $M4$ ; circles— $M5$ . The curves are theoretical. 1—Model (1) for  $M5$  with  $\beta=0.41$ ; 2—model (1) for  $M4$  with  $\beta=0.23$ ; 3—low-temperature region for  $M2$  according to model (1) with  $\beta=0.1$ ; 4—model (1) for  $M3$  with  $\beta=1.0$ ; 5—2D Ising model (2) for  $M2+M3$ .

and  $M3$  can apparently be described in the approximation of a 2D model (Fig. 5).

For the sample with  $x=0.23$  the low-temperature region for components  $M2$  and  $M3$ , over the range 4–200 K, can be described satisfactorily by the 2D approximation (Fig. 6). For both  $M2$  and  $M3$  we find  $\beta=0.1$  and

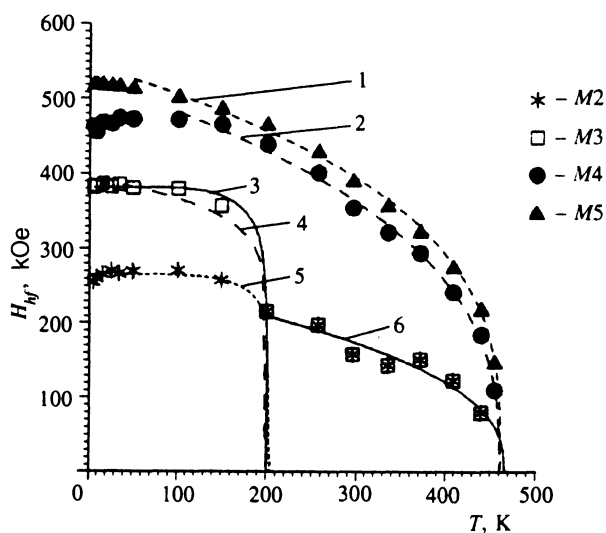


FIG. 6. Temperature dependence of the fields  $H_{hf}(Mi)$  for a  $YBa_2(Cu_{0.77}Fe_{0.23})_3O_{6.49}$  sample. The points are experimental. Asterisks—Component  $M2$ ; squares— $M3$ ; circles— $M4$ ; triangles— $M5$ . The curves are theoretical. 1—Model (1) for  $M5$  with  $\beta=0.35$ ; 2—model (1) for  $M4$  with  $\beta=0.31$ ; 3—low-temperature region for  $M3$  according to the 2D Ising model in (2); 4—the same, according to model (1) with  $\beta=0.1$ ; 5—low-temperature region for  $M2$  according to the 2D Ising model in (2); 6—Model (1) for  $M2+M3$  with  $\beta=40$ .

$T_{N1}=200$  K in model (1). In even better agreement with the experimental data is the theoretical curve corresponding to the 2D Ising model, (2), with  $T_{N1}=200$  K and  $J_1=J_2=88$  K. For both components, the region  $200 < T < T_{N2}$  is described satisfactorily by model (1) with the values  $\beta=0.40$  and  $T_{N2}=466$  K.

#### 4. DISCUSSION OF RESULTS

In discussing the type and dimensionality of the magnetic order, we made use of the following considerations. The behavior of a magnetic system is characterized by the dimensionality  $d$  of the magnetic lattice and by the dimensionality of the order parameter  $n$  (Ref. 19, for example). The parameter  $d$  can take on values of 1 (in the case of 1D chains), 2 (a layered structure or a surface), and 3 (a bulk material). The order parameter  $n$  is determined by the particular model used to describe the magnetic system, i.e., by the type of Hamiltonian. For  $n=1$  (the Ising model) we would have  $H=-\sum J_{ij}S_i^zS_j^z$ ; for  $n=2$  (the XY planar model) we would have  $H=-\sum_{ij}(S_i^xS_j^x+S_i^yS_j^y)$ ; and for  $n=3$  (the Heisenberg model) we would have  $H=-\sum J_{ij}\mathbf{S}_i\mathbf{S}_j$ . For all values of  $n$ , long-range order exists only in the case  $d=3$ . The Ising model ( $n=1$ ) allows 2D and 3D long-range orders. In the Heisenberg model ( $n=1$ ) and the XY model ( $n=2$ ), there is no low-dimensionality ( $d=1$  or 2) order. According to the model of critical coefficients, the parameter  $\beta$  can take on the following values:<sup>16</sup>

$n$	$d=3$			$d=2$	Molecular-field model
	1	2	3	1	
$\beta$	0.31	0.33	0.35	0.125	0.5

##### 4.1. Oxygen-rich samples

The components  $M1$  and  $M2$  belong to  $\text{Fe}^{3+}$  ions with an intermediate spin value,  $S=3/2$  (IS), in Cu1 sites with plane-square coordination ( $k=4$ ) and square-pyramid coordination ( $k=5$ ), respectively.<sup>13,20</sup> Coordinations with  $k=4$  are present only within twin domains, while coordinations with  $k=5$  can form both inside domains (Fe-Fe dimers and larger clusters) and at domain walls.

**Component M1.** The temperature dependence  $H_{\text{hf}}(M1)=f(T)$  is approximately linear. The lines in the Mössbauer spectrum are greatly broadened. These results suggest that the iron ions corresponding to component  $M1$  are in a spin-glass (SG) order. A linear dependence of the field-induced magnetization  $M(T)$  was found and derived theoretically in Refs. 21–23 for concentrated spin glasses. A similar temperature dependence for the fields  $H_{\text{hf}}$  with greatly broadened spectral lines was observed by Wagner and Gonser<sup>24</sup> and also by Meyer *et al.*<sup>25</sup> for a AuFe alloy, which is a classic example of a spin glass. Interestingly, the temperature of the magnetic ordering found from Mössbauer data in those studies is about 20% higher than the spin freezing temperature  $T_F$  found from measurements of the magnetic susceptibility. We are apparently seeing a similar effect for the  $M1$  component.

**Component M2.** The temperature dependence  $H_{\text{hf}}(M2)=f(T)$  indicates 3D long-range order, probably

of Heisenberg type. Sites with  $k=5$  can form both within twin domains and at the edges of domain walls. A 3D long-range magnetic order can apparently arise in the Cu1 sublattice by the following two mechanisms:

1. Exchange interactions between Cu1 planes inside twin domains in the superconducting state can occur only through superconduction electrons of the intermediate Cu2 layers.

2. The domain walls may include some of the copper ions from Cu2 planes, which are not participating in the superconductivity and which mediate a superexchange interaction along the  $z$  axis in a Fe(Cu1)–O–Cu2–Cu2–O–Cu1 chain.

Eibschutz and Lines<sup>26</sup> have shown that  $\text{Fe}^{3+}$  ions with intermediate spin  $S=3/2$  and  $k=5$  oxygen coordination cannot form long-range magnetic order. The reason is that in this coordination the  $\sigma$  bonds of  $3d$  electrons do not take part in an exchange interaction. In this case, mechanism (1) is more likely for the formation of long-range magnetic order with  $k=5$ .

In the semiconducting sample with  $x=0.23$ , a 3D long-range magnetic order is characteristic of the  $M1+M2$  components. The magnetic Cu2 sublattice apparently has a significant effect on the state of the Cu1 sites upon the loss of superconductivity, and a 3D magnetic order forms in Cu1 sites within domains by mechanism (2).

**Component M4.** The temperature dependence  $H_{\text{hf}}(M4)$  clearly points to a 2D magnetic order of the Ising type. Component  $M4$  belongs to iron ions in Cu1 sites with the sixfold oxygen coordination of a complete octahedron<sup>14,17</sup> ( $k=6$ ). Sites of this type form primarily at domain walls.<sup>27</sup> A 2D order of these sites agrees with the proposition that iron ions with  $k=6$  at domain walls form magnetic chains along [110] directions in the  $ab$  plane. If the domain wall is thick enough, these chains can grow into 2D magnetic clusters in the  $ab$  plane. Such a magnetic structure is in agreement with the model of Ref. 26, from which it follows that a long-range 2D magnetic order is possible for Cu1 sites with  $k=6$ . As the iron concentration is increased, the number of these clusters (or their size) increases slightly, as is indicated by the increase in the relative intensity  $S_{\text{rel}}$  of component  $M4$ :  $S_{\text{rel}}(M4) \approx 7\%$ , 16%, and 23% for  $x=0.01$ , 0.10, and 0.23, respectively.

Our data agree only partially with the results of Ref. 28, where an attempt was made to describe all experimental curves of  $H_{\text{hf}}(Mi)=f(T)$  for  $x=0.1$  by means of a quasi-1D Ising model.

**Component M5.** This component, with a high magnetic-ordering point,  $T_{m2} \approx 400$  K, appears in the samples with  $x > 0.15$ , in which the superconductivity is suppressed by the high iron content. This component corresponds to high-spin  $\text{Fe}^{3+}$  ions in Cu2 sites. The  $H_{\text{hf}}(M5)=f(T)$  behavior supports the conclusion, reached on the basis of neutron diffraction data,<sup>29</sup> that there is 3D magnetic order in the Cu2 sublattice in the normal phase.

## 4.2. Oxygen-poor samples

*Components M4 and M5.* The behavior of the  $H_{\text{hf}}(M4)$  and  $H_{\text{hf}}(M5)$  curves is evidence of 3D long-range order for high-spin  $\text{Fe}^{3+}$  ions in Cu1 and Cu2 sites. In view of the Ising nature of the magnetic order ( $n=1$ ) of the *M4* component for the oxygen-rich samples, it is logical to suggest that the Ising order persists after the oxygen is removed, since the oxygen coordination of sites of this type does not change. This conclusion is also indicated by the value  $\beta=0.31$  for  $x=0.23$ , which corresponds to the exact theoretical value for the 3D Ising model. Consequently, the loss of superconductivity leads to a superexchange between Cu1 sites in accordance with the mechanism (2) involving magnetic copper ions in Cu2 layers. However, the value  $\beta=0.23$  for the *M4* component of the sample with  $x=0.1$  apparently means that 2D clusters exist again in this case. For  $x=0.01$ , the  $H_{\text{hf}}(M4)=f(T)$  curve is typical of 2D order with  $\beta \approx 0.1$ .

Of particular interest is the behavior of component *M5*, which is linked with iron ions in Cu2 sites. As was mentioned earlier, this component is missing from the superconducting samples. It arises only after the superconductivity is lost either through the removal of oxygen or through doping with iron to a high concentration. Where are the peaks from iron ions in Cu2 sites in the spectra of the oxygen-saturated samples? Analysis of the spectra of a specific sample with  $x=0.1$  reveals the following: In the superconducting state, component *M5* is not present in the low-temperature spectra split by the magnetic hyperfine interaction. After oxygen is removed, on the other hand, the area of this component,  $S_{\text{rel}}(M5)$ , amounts to about 25% of the total area of the spectrum. This result suggests that resonant lines from  $^{57}\text{Fe}$  nuclei in Cu2 sites in the superconducting state merge with the spectrum from Cu1 sites and that the field  $H_{\text{hf}}$  for the Cu2 sites is at most  $\approx 270$  kOe, a value characteristic of low-spin states of  $\text{Fe}^{3+}$  ions. The increase in the field  $H_{\text{hf}}$  in the component *M5* to  $\approx 510$  kOe after the loss of superconductivity is unambiguous evidence that the iron ions in Cu2 sites undergo a transition from a low-spin state (LS) to a high-spin state (HS). A strong exchange interaction arises between magnetic  $\text{Fe}(\text{Cu}2)$  ions and  $\text{Fe}^{3+}$  ions in domain walls (component *M4*). As a result, the temperature dependence for *M5* is similar to that for *M4* and is characteristic of 3D order.

*Crossover effect for components M2 and M3.* When the superconductivity is lost as the oxygen is removed, the component *M1+M2* is transformed into component *M2+M3*, with a higher field  $H_{\text{hf}}$ . The apparent reason for the increase in  $H_{\text{hf}}$  is an increase in the spin state of the iron ions (an LS  $\rightarrow$  HS transition), as is observed for component *M5*. The magnetic state of the Cu1 sites is being strongly influenced by the Cu2 sublattice, and the temperature of the transition to the paramagnetic state for the Cu1 sites moves off to the Néel point of the Cu2 sublattice. The curves of  $H_{\text{hf}}=f(T)$  for *M2* and *M3* are very complicated, defying description by any single model over the entire temperature range. The temperature dependence of  $H_{\text{hf}}$  is governed by the set of exchange interactions within the

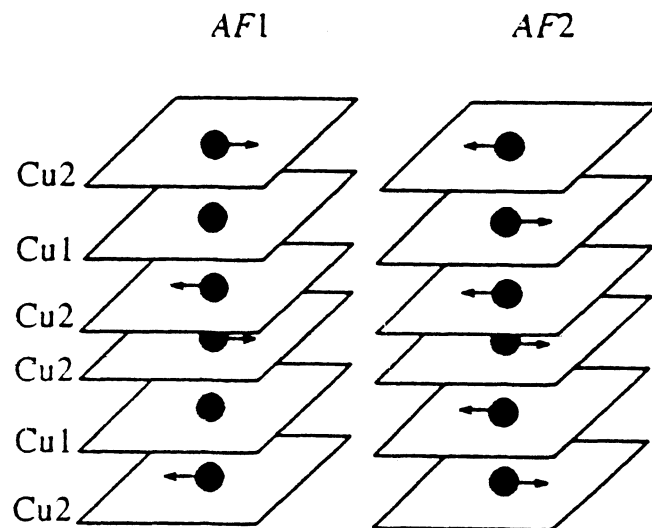


FIG. 7. Schematic diagram of the magnetic structure of the *AF1* and *AF2* phases. In *AF1*, only the Cu2 sublattice has an antiferromagnetic order. In the *AF2* phase, with an *AF* order of the Cu1 sublattice, Cu2 sites can be ordered either antiferromagnetically or ferromagnetically.

Cu1 sublattice and between the Cu1 and Cu2 sublattices.

The  $H_{\text{hf}}(T)$  behavior can be explained on the basis of particular features of the ordering of the copper Cu1 and Cu2 sublattices upon doping. These features were studied theoretically in Ref. 30 for  $\text{YBa}_2\text{Cu}_3\text{O}_{6+t}$  and have been observed experimentally by neutron diffraction<sup>31,32</sup> for the  $\text{YBa}_2\text{Cu}_{2.8}\text{Co}_{0.2}\text{O}_{6+y}$  system. According to Ref. 30, at  $t=0$  the  $\text{CuO}_2$  planes contain only magnetic  $\text{Cu}^{2+}$  ions, and the Cu1 sites contain only nonmagnetic  $\text{Cu}^{1+}$  ions. The result is a 3D order of the spins in Cu2 sites. With increasing  $t$ , the holes which form put the copper ions in Cu1 sites in a magnetic  $\text{Cu}^{2+}$  state. As a result of the competition between the antiferromagnetic interactions of neighboring Cu2 layers (Cu2–Cu2) and Cu2–O–Cu1–O–Cu2 superexchange ferromagnetic interactions, a system with frustrated bonds forms (Fig. 7). Any impurity magnetic ions can play the role of magnetic copper ions in Cu1 sites. Accordingly, several types of magnetic order can be established at low temperatures, depending on the relations between the exchange integrals for the different types of interactions in the system. As the temperature is raised, the system generally becomes a Heisenberg system with a single type of 3D order.

One might suggest that, in our samples with  $x=0.1$ , component *M3* in Cu1 sites has frustrated bonds and acquires a spin-glass order at low temperatures (Fig. 5). For component *M2*, a 2D order is characteristic at low temperatures. As the temperature is raised, the transition from the *SG* and 2D phases to a paramagnetic phase occurs through 2D ordering (Fig. 5). In the sample with  $x=0.23$  the size of the magnetic clusters increases because of the high iron content. At low temperatures, the result is a transformation of the *SG* state into a long-range 2D magnetic order of the Ising type for both *M2* and *M3* (Fig. 6).

As the temperature is raised, the system becomes more nearly isotropic (corresponding to the Heisenberg model), and 3D order is observed. In both cases we are thus seeing a crossover, i.e., a transition from one dimensionality of the magnetic lattice or of the magnetic order parameter to another. In our case, a  $3n \rightarrow 1n$  and/or  $2n \rightarrow 1n$  crossover is apparently possible as  $T \rightarrow 0$ .

A similar picture of the magnetic order has been observed experimentally in a neutron-diffraction study of the  $\text{YBa}_2\text{Cu}_{2.8}\text{Co}_{0.2}\text{O}_{6+y}$  system.<sup>31,32</sup> For  $0.37 \leq y < 0.8$ , two types of magnetic order were found: *AF1*, associated with an ordering of copper ions exclusively in the Cu2 sublattice, and *AF2*, in which case copper ions in Cu1 sites also participate (Fig. 7). As the temperature is varied, one type of order may give way to the other. For  $y=0.45$ , both types of order exist at low temperatures, but *AF2* disappears at  $T \approx 200$  K.

In our test samples, the behavior of components *M2* and *M3* is apparently governed by the existence of *AF1* and *AF2* magnetic phases and a competition between Cu2–Cu2 and Cu2–O–Cu1 exchange interactions. The weakening of the second of these interactions with increasing temperature results in a transformation of the *AF1* and *AF2* phases and is accompanied by a crossover in the order parameter. We apparently are observing a transition from the *AF2* phase to *AF1* at the crossover point.

The behavior of *M5* (and of the related *M4*) is governed primarily by the *AF1* phase, which is due to an ordering of the Cu2 sublattice.

## 5. CONCLUSION

**Cu2 sites.** The iron ions in the superconducting samples are in a low-spin state (we call this induced diamagnetism at paramagnetic ions due to the superconductivity); when the superconductivity is suppressed, they go into a high-spin  $\text{Fe}^{3+}$  state ( $S=5/2$ ). The magnetic order of the  $\text{Fe}^{3+}$  ions is 3D order, in accordance with the antiferromagnetic 3D order of the Cu2 sublattice.

**Cu1 sites.** The iron ions within domains with  $k=4$  have frustrated exchange bonds. In the superconducting region their magnetic state is similar to a spin-glass state. In the  $k=5$  coordination the iron ions exhibit a 3D order in the superconducting region, indicating that superconduction electrons of Cu2 layers may be involved in the creation of a 3D magnetic order in the Cu1 sublattice. The same conclusion is a possibility for the  $k=4$  coordination.

When the superconductivity is suppressed, the spin state of the iron ions in the  $k=4$  and  $k=5$  coordinates increases. At low temperatures the magnetic state of these sites can be described by either a 2D or *SG* order, depending on the iron concentration. As the temperature is raised, a crossover is observed: the *SG* and 2D magnetic orders convert into a paramagnetic state through a 3D Heisenberg order.

The anomalies on the  $H_{\text{hf}}(T)$  curves in the interval 150–200 K are apparently due to weakening of the exchange interactions within the Cu1 sublattice and a transition of the *AF2* phase into *AF1*, accompanied by the dis-

appearance of the long-range magnetic order in the Cu1 sublattice. This transition is accompanied by a crossover in the order parameter.

The  $\text{Fe}^{3+}$  ions with  $k=6$  form clusters in the domain walls. These clusters are linear magnetic chains along [110] axes. If the domain wall is thick enough, these chains grow into 2D magnetic clusters in the *ab* plane. In the superconducting state, one observes 2D magnetic order for sites of this type, with the low value  $T_{m1} \sim 20$  K. When the superconductivity is suppressed, superexchange interactions of these clusters with the Cu2 sublattice along the *c* axis arise, and the magnetic order approaches 3D order. The spin state of the  $\text{Fe}^{3+}$  ions in these sites apparently remains the same.

We are deeply indebted to L. E. Li for assistance in the computer analysis of the experimental results and to A. K. Zvezdin for a useful discussion of the results.

- <sup>1</sup>Z. Q. Qiu *et al.*, *J. Magn. Magn. Mater.* **69**, L221 (1987).
- <sup>2</sup>X. Z. Zhou *et al.*, *Phys. Rev. B* **36**, 7230 (1987).
- <sup>3</sup>I. S. Lyubutin *et al.*, *JETP Lett.* **47**, 196 (1988).
- <sup>4</sup>T. Tamaki *et al.*, *Solid State Commun.* **65**, 43 (1988).
- <sup>5</sup>I. Nowik *et al.*, *Phys. Rev. B* **38**, 6677 (1988).
- <sup>6</sup>I. S. Lyubutin and V. G. Terziev, *Progress in High Temperature Superconductivity*, ed. by Y. Murakami (World Scientific, Singapore, 1989), Vol. 21, p. 281.
- <sup>7</sup>S. Nasu *et al.*, *Progress in High Temperature Superconductivity*, ed. by Y. Murakami (World Scientific, Singapore, 1989), Vol. 15, p. 214.
- <sup>8</sup>Z. Q. Qiu *et al.*, *J. Magn. Magn. Mater.* **78**, 359 (1989).
- <sup>9</sup>I. S. Lyubutin, *Nucl. Instrum. Methods B* **76**, 276 (1993).
- <sup>10</sup>A. M. Balagurov *et al.*, *Sverkhprovodimost' (KIAE)* **3**(4), 615 (1990) [*Superconductivity* **3**(4), 580 (1990)].
- <sup>11</sup>I. S. Lyubutin *et al.*, *Sverkhprovodimost' (KIAE)* **3**(14), 2350 (1990) [*Superconductivity* **3**(14), 5424 (1990)].
- <sup>12</sup>I. S. Lyubutin *et al.*, *Sverkhprovodimost' (KIAE)* **5**(8), 1423 (1992) [*Superconductivity* **5**(8), 1396 (1992)].
- <sup>13</sup>I. S. Lyubutin *et al.*, *Sverkhprovodimost' (KIAE)* **5**(10), 1842 (1992) [*Superconductivity* **5**(10), 1757 (1992)].
- <sup>14</sup>T. Tamaki *et al.*, *Hyperfine Interact.* (1994).
- <sup>15</sup>I. S. Lyubutin *et al.*, *Physica C* **195**, 383 (1992).
- <sup>16</sup>L. J. De Jongh, *Magnetic Properties of Layered Transition Metal Compounds*, ed. by L. J. De Jongh (Kluwer Academic, Netherlands, 1990), pp. 1–51.
- <sup>17</sup>I. S. Lyubutin *et al.*, *Physica C* **199**, 296 (1992).
- <sup>18</sup>D. Hechel *et al.*, *Phys. Rev. B* **42**, 2166 (1990).
- <sup>19</sup>J.-P. Renard, *Organic and Inorganic Low-Dimensional Crystalline Materials*, ed. by P. Delhaes and M. Drillon (Plenum, New York, 1987), p. 125.
- <sup>20</sup>M. E. Lines and M. Eibschutz, *Physica C* **166**, 235 (1990).
- <sup>21</sup>S. B. Liao, *J. Appl. Phys.* **63**, 4354 (1988).
- <sup>22</sup>E. M. Jackson *et al.*, *J. Magn. Magn. Mater.* **80**, 229 (1989).
- <sup>23</sup>M. Lubecka and L. J. Maksymowicz, *Phys. Rev. B* **44**, 10106 (1991).
- <sup>24</sup>H. G. Wagner and U. Gonser, *J. Magn. Magn. Mater.* **31–34**, 1343 (1983).
- <sup>25</sup>C. Meyer *et al.*, *J. Magn. Magn. Mater.* **46**, 254 (1985).
- <sup>26</sup>M. E. Eibschutz and M. E. Lines, *Phys. Rev. B* **38**, 8858 (1988).
- <sup>27</sup>I. S. Lyubutin, *Physica C* **182**, 315 (1991).
- <sup>28</sup>W. Peng *et al.*, *Physica C* **169**, 23 (1990).
- <sup>29</sup>J. M. Tranquada *et al.*, *Phys. Rev. B* **38**, 2477 (1988).
- <sup>30</sup>Y. Lu and B. R. Patton, *J. Phys. Cond. Matt.* **2**, 9423 (1990).
- <sup>31</sup>R. F. Miceli *et al.*, *Phys. Rev. B* **38**, 9209 (1988).
- <sup>32</sup>R. F. Miceli *et al.*, *Phys. Rev. B* **39**, 12374 (1989).

Translated by D. Parsons